Published OnlineFirst July 17, 2012; DOI: 10.1158/1940-6207.CAPR-11-0397

Research Article

Cancer Prevention Research

# Taxifolin Suppresses UV-Induced Skin Carcinogenesis by Targeting EGFR and PI3K

Naomi Oi[1], Hanyong Chen[1], Myoung Ok Kim[1,2], Ronald A. Lubet[3], Ann M. Bode[1], and Zigang Dong[1]

## Abstract

Skin cancer is one of the most commonly diagnosed cancers in the United States. Taxifolin reportedly exerts multiple biologic effects, but the molecular mechanisms and direct target(s) of taxifolin in skin cancer chemoprevention are still unknown. *In silico* computer screening and kinase profiling results suggest that the EGF receptor (EGFR), phosphoinositide 3-kinase (PI3K), and Src are potential targets for taxifolin. Pull-down assay results showed that EGFR, PI3K, and Src directly interacted with taxifolin *in vitro*, whereas taxifolin bound to EGFR and PI3K, but not to Src in cells. ATP competition and *in vitro* kinase assay data revealed that taxifolin interacted with EGFR and PI3K at the ATP-binding pocket and inhibited their kinase activities. Western blot analysis showed that taxifolin suppressed UVB-induced phosphorylation of EGFR and Akt, and subsequently suppressed their signaling pathways in JB6 P+ mouse skin epidermal cells. Expression levels and promoter activity of COX-2 and prostaglandin $E_2$ ($PGE_2$) generation induced by UVB were also attenuated by taxifolin. The effect of taxifolin on UVB-induced signaling pathways and $PGE_2$ generation was reduced in EGFR knockout murine embryonic fibroblasts (MEF) compared with EGFR wild-type MEFs. Taxifolin also inhibited EGF-induced cell transformation. Importantly, topical treatment of taxifolin to the dorsal skin significantly suppressed tumor incidence, volume, and multiplicity in a solar UV (SUV)-induced skin carcinogenesis mouse model. Further analysis showed that the taxifolin-treated group had a substantial reduction in SUV-induced phosphorylation of EGFR and Akt in mouse skin. These results suggest that taxifolin exerts chemopreventive activity against UV-induced skin carcinogenesis by targeting EGFR and PI3K. *Cancer Prev Res; 5(9); 1103–14. ©2012 AACR.*

## Introduction

Skin cancer is one of the most common cancers in the United States. Each year, more than 1,000,000 new cases of skin cancers are reported in the United States, making up 40% of all diagnosed cancers (1). Chronic UV exposure is recognized as a major etiologic factor of skin carcinogenesis (2). The UV spectrum can be divided into 3 wavelengths, UVA (320–400 nm), UVB (280–320 nm), and UVC (200–280 nm; refs. 3, 4). Although UVC is filtered out by the ozone layer, UVA and UVB reach the surface of the earth. Of the UV irradiation that reaches the surface of the earth, 90% to 99% is composed of UVA and 1% to 10% is composed of UVB (4). UVA is carcinogenic and causes photoaging and wrinkling of the skin (5). UVB is mainly responsible for a variety of skin diseases including melanoma and nonmelanoma skin cancers because it is capable of triggering the initiation, promotion, and progression phases of skin cancer (6, 7). Therefore, targeting UV-induced signaling might be an effective strategy for preventing skin carcinogenesis.

The EGF receptor (EGFR) is activated by UV radiation (8). EGFR is a member of the receptor tyrosine kinase, and is reported to be activated and/or overexpressed in a variety of human cancers including UV-induced skin cancer (9, 10). UV irradiation rapidly activates EGFR through the induction of EGFR ligands and the inactivation of cytoplasmic protein tyrosine phosphatases that maintains low basal levels of phosphorylated EGFR (11–13). UV-activated EGFR in turn activates a number of signaling cascades, including extracellular signal–regulated kinases (ERK), p38 kinase, and c-*jun*-$NH_2$-kinase (JNK), which are known regulators of cell division (14–16). In response to UV irradiation, EGFR also activates phosphoinositide 3-kinase (PI3K), leading to Akt activation and suppression of apoptosis (17). Therefore, the EGFR and PI3K/Akt signaling pathways are logical molecular targets for chemoprevention of UV-induced skin cancer.

Taxifolin, also known as dihydroquercetin, is a flavonone commonly found in onions (18), milk thistle (19), French

**Authors' Affiliations:** [1]The Hormel Institute, University of Minnesota, Austin, Minnesota; [2]School of Animal Science and Biotechnology, Kyungpook National University, Sangju, Korea; and [3]National Cancer Institute, Bethesda, Maryland

**Note:** Supplementary data for this article are available at Cancer Prevention Research Online (http://cancerprevres.aacrjournals.org/).

**Corresponding Author:** Zigang Dong, The Hormel Institute, University of Minnesota, 801 16th Ave NE, Austin, MN 55912. Phone: 507-437-9600; Fax: 507-437-9606; E-mail: zgdong@hi.umn.edu

**doi:** 10.1158/1940-6207.CAPR-11-0397

Published OnlineFirst July 17, 2012; DOI: 10.1158/1940-6207.CAPR-11-0397



maritime bark (20), and Douglas fir bark (21) in an aglycone or glycoside form. Taxifolin has multiple biologic effects, including antioxidant and anti-inflammatory effects, and plays a role in preventing cardiovascular disease (22–24). Recently, several studies have focused on taxifolin as a potential cancer chemopreventive agent. One study showed that aglycone form of taxifolin exerts chemopreventive effects through an antioxidant response element (ARE)-dependent mechanism in colon cancer cells (25). The taxifolin aglycone form is also reported to induce apoptosis in prostate cancer cells (26). Although these reports provide evidence that taxifolin might exert chemopreventive effects against several cancers, the molecular mechanisms and direct targets of taxifolin are still unclear. Herein, we report that taxifolin suppresses UVB-induced activation of signal transduction by directly inhibiting EGFR and PI3K in JB6 P+ mouse skin epidermal cells. Moreover, taxifolin strongly suppresses tumor incidence in a solar UV (SUV)-induced skin carcinogenesis mouse model. Thus, taxifolin acts as an inhibitor of EGFR and PI3K and is expected to have beneficial effects in the prevention of UV-induced skin carcinogenesis.

## Materials and Methods

### Chemicals

The aglycone form of taxifolin was purchased from Sigma-Aldrich [>85%; 2*R*,3*R*-(+)-taxifolin] for *in vitro* and cell-based experiments; for the animal study, taxifolin was purchased from ENZO Life Sciences (> 90%; (+)-taxifolin). Active EGFR, PI3K (p110δ/p85α), and Src proteins were from Millipore. The antibody to detect phosphorylated p38 (Tyr180/Tyr182) was purchased from BD Biosciences. Antibodies against total Src, p38, ERK1/2, JNKs, Akt, p90RSK, and EGFR, and phosphorylated ERK1/2 (Thr202/Tyr204), JNKs (Thr183/Tyr185), Akt (Tyr308 and Ser473), MSK (Ser376), p90RSK (Thr359/Ser363), and EGFR (Tyr1068) were from Cell Signaling Biotechnology. The antibodies against total MSK, PI3K (p110), and β-actin were obtained from Santa Cruz Biotechnology. The prostaglandin $E_2$ ($PGE_2$) EIA Kit, COX Inhibitor Screening Assay Kit, and antibody against COX-2 were purchased from Cayman Chemical.

### Cell culture and transfection

The JB6 P+ mouse epidermal cell line was purchased from American Type Culture Collection and cultured in Eagle's Minimum Essential Medium (MEM)/5% FBS. For the luciferase assay, the JB6 P+ cells were stably transfected with a COX-2 luciferase reporter plasmid and maintained in MEM/5% FBS containing 200 μg/mL G418 as described earlier (27). EGFR wild-type (EGFR/WT) and EGFR knockout (EGFR/KO) murine embryonic fibroblasts (MEF) were cultured in Dulbecco's modified Eagle's medium (DMEM)/10% FBS as reported previously (28). All cells were cultured with antibiotics at 37°C in a $CO_2$ incubator. Cells were cytogenetically tested and authenticated before the cells were frozen. Each vial of frozen cells was thawed and maintained for a maximum of 8 weeks.

### *In silico* target identification

To find the potential biologic targets of taxifolin, a shape similarity method, a part of the PHASE module of Schrödinger (29) molecular modeling software package, was used on the basis of the chemical structure of taxifolin. The parameter of atom-type for volume was set to pharmacophore, which means that the queries were used not only to consider shape similarity but also to align potential pharmacophore points with the targets. The protein target library was obtained from the Protein Data Bank (PDB; ref. 30). To provide more structure orientations for the possible alignment, we set the maximum number of conformers per molecule in the library to be generated at 100 while retaining up to 10 conformers per rotatable bond. We filtered out the conformers with similarity below 0.7. Then, we obtained the PDB ID associated with each aligned target molecule. The PDB ID could show us the protein type through the online Protein Data Bank.

### Pull-down assays

Taxifolin-conjugated sepharose 4B beads or sepharose 4B beads were prepared as reported earlier (27). For *in vitro* or *ex vivo* pull-down assay, active EGFR, PI3K, or Src (200 ng) or lysates from JB6 P+ cells (500 μg) were mixed with 50 μL of taxifolin-conjugated sepharose 4B beads or sepharose 4B beads in reaction buffer [50 mmol/L Tris–HCl (pH 7.5), 5 mmol/L EDTA, 150 mmol/L NaCl, 1 mmol/L dithiothreitol (DTT), 0.01% NP-40, 2 μg/mL bovine serum albumin, 0.02 mmol/L phenylmethylsulfonylfluoride (PMSF), and 1× protease inhibitor cocktail]. After incubation with gentle rocking at 4°C overnight, the beads were washed 5 times with washing buffer [50 mmol/L Tris–HCl (pH 7.5), 5 mmol/L EDTA, 150 mmol/L NaCl, 1 mmol/L DTT, 0.01% NP-40, and 0.02 mmol/L PMSF], and then the proteins bound to the beads were analyzed by Western blotting. For the ATP competition assay, active EGFR or PI3K (200 ng) was incubated with different concentrations of ATP (0, 10, or 100 μmol/L) in reaction buffer at 4°C overnight. Taxifolin-conjugated sepharose 4B beads or sepharose 4B beads were added and again incubated at 4°C overnight. After washing 5 times with washing buffer, the proteins bound to the beads were analyzed by Western blotting.

### *In vitro* EGFR kinase assay

The *in vitro* EGFR kinase assay was carried out in accordance with the instructions provided by Millipore. Active EGFR (100 ng) was mixed with taxifolin (0, 20, 40, or 80 μmol/L) or erlotinib (10 μmol/L, LC laboratories) in reaction buffer [40 mmol/L MOPS/NaOH (pH 7.0), 1 mmol/L EDTA, 10 mmol/L $MnCl_2$, and 0.8 mol/L ammonium sulphate]. Erlotinib, a well-known EGFR inhibitor, was used as a positive control. The mixture was incubated with 500 μmol/L angiotensin II for 5 minutes at room temperature followed by incubation with 10 μL of a ATP mixture [25 mmol/L MgAc and 0.25 mmol/L ATP-containing 10 μCi [$\gamma$-$^{32}$P]ATP] for 20 minutes at 30°C and then 25 μL of reaction mixture were transferred onto P81 papers.

Published OnlineFirst July 17, 2012; DOI: 10.1158/1940-6207.CAPR-11-0397



The papers were washed with 1% phosphoric acid twice and with acetone once. The radioactive incorporation was determined using a scintillation counter.

### *In vitro* PI3K kinase assay

The *in vitro* PI3K kinase assay was carried out as described earlier (31). Active PI3K (100 ng) was incubated with taxifolin (0, 20, 40, or 80 μmol/L) or LY294002 (10 μmol/L) for 10 minutes at 30°C. LY 294002, a well-known PI3K inhibitor, was used as a positive control. The mixtures were incubated with 0.5 mg/mL phosphatidylinositol (MP Biomedicals) for 5 minutes at room temperature, followed by incubation with reaction buffer [10 mmol/L Tris-HCl (pH 7.6), 60 mmol/L $MgCl_2$, and 0.25 mmol/L ATP containing 10 μCi [$\gamma$-$^{32}$P] ATP] for an additional 10 minutes at 30°C. The reaction was stopped by adding 15 μL of 4 N HCl and 130 μL of chloroform: methanol = 1:1. After mixing, the lower chloroform phase were spotted onto a silica gel plate (Merck KGaA). The resulting $^{32}$P-labeled phosphatidylinositol-3-phosphate (PI3P) was separated by thin layer chromatography with developing solvent (chloroform: methanol:$NH_4OH$:$H_2O$ = 60:47:2:11.3) and then visualized by autoradiography.

### Molecular modeling

The active wild-type EGFR tyrosine kinase domain (PDB ID:1m17) was chosen for docking studies. Its X-ray diffraction structure had a resolution of 2.6 å (32), and erlotinib was bound to the ATP-binding site of the EGFR. For PI3K, the crystal structure of the murine P110-δ in complex with ZSTK474 (PDB ID:2WXL) was chosen for docking studies. Its X-ray diffraction structure had a resolution of 1.99 å. ZSTK474 is an ATP-competitive inhibitor and has a shape similarity with taxifolin of 0.67 (33). EGFR and PI3K were prepared for docking using the Protein Preparation Wizard in the Schrödinger Suite 2010 by a standard procedure outlined separately. Taxifolin was prepared using MacroModel of Schrödinger and minimized, and the lowest energy conformations for docking were determined by using default parameters. The protein-ligand docking analysis was conducted using the Induced Fit docking program of Schrödinger, which can provide the ligand binding flexibility with the binding pocket residues. Images are generated with the UCSF Chimera program (34).

### Cell viability assay

JB6 P+ cells ($1 \times 10^4$) were cultured in 96-well plates and then treated with various concentrations of taxifolin (0, 20, 40, or 80 μmol/L). After incubation for 24, 48, or 72 hours, 20 μL of CellTiter96 Aqueous Non-Radioactive Cell Proliferation Assay Kit (Promega) were added to each well. After additional incubation for 1 hour at 37°C in a 5% $CO_2$ incubator, absorbance was measured at 490 and 690 nm.

### UVB irradiation

A UVB irradiation system (FS20 T12/UVB, National Biological corporation) was used to stimulate cells in the serum-free medium. The spectral peak from the UVB source was at 311 nm.

### Western blotting

JB6 P+ cells ($1 \times 10^6$) or MEFs ($5 \times 10^5$) were cultured in 10-cm dishes and then starved in serum-free medium for 48 hours. The cells were treated with various concentrations of taxifolin (0, 20, 40, or 80 μmol/L), gefitinib (2 μmol/L), and/or LY294002 (2 μmol/L) for 24 hours before exposure to UVB (4 kJ/m$^2$). The lysate proteins were subjected to SDS-PAGE and transferred to a polyvinylidene difluoride (PVDF) membrane. After blocking with 5% milk, the membrane was incubated with a specific primary antibody, and then protein bands were visualized by the ECL system after hybridization with a horseradish peroxidase–conjugated secondary antibody.

### *COX-2* luciferase assay

JB6 P+ cells stably transfected with a COX-2 luciferase reporter plasmid ($8 \times 10^3$) were cultured in 96-well plates and then starved in serum-free medium for 24 hours. The cells were treated with various concentrations of taxifolin (0, 20, 40, or 80 μmol/L) for 1 hour before exposure to UVB (4 kJ/m$^2$). After incubation for 12 hours, the cells were disrupted with 100 μL of lysis buffer [0.1 mol/L potassium phosphate buffer (pH 7.8), 1% Triton X-100, 1 mmol/L DTT, and 2 mmol/L EDTA], and luciferase activity was measured using a luminometer (Luminoskan Ascent; Thermo Election).

### $PGE_2$ assay

JB6 P+ cells or MEFs ($1 \times 10^5$) were cultured in 6-well plates and then starved in serum-free medium for 24 hours. The cells were treated with various concentrations of taxifolin (0, 20, 40, or 80 μmol/L) or celecoxib (10 μmol/L) for 1 hour before exposure to UVB (4 kJ/m$^2$). After incubation for 6 hours, the amount of $PGE_2$ released into the medium was measured using the $PGE_2$ EIA kit following the supplier's instructions. A standard curve with $PGE_2$ provided with the kit was generated at the same time. Celecoxib, a well-known inhibitor for COX-2, was used as a positive control.

### *In vitro* COX-2 activity

*In vitro* COX-2 activity was determined by measuring the synthesis of PGs using the COX Inhibitor Screening Assay Kit following the supplier's instructions. A standard curve with PGs was generated at the same time. Celecoxib was used as a positive control.

### Cell transformation assay

JB6 P+ cells ($8 \times 10^3$) were suspended in 1 mL of BME supplemented with 10% FBS and 0.33% agar and treated with various concentrations of taxifolin (0, 20, 40, or 80 μmol/L), gefitinib (0.1 μmol/L), LY294002 (1 μmol/L), or celecoxib (10 μmol/L) together with 1 ng/mL EGF on 3 mL of solidified Basel Medium Eagle supplemented with 10% FBS and 0.5% agar with the indicated concentrations

Published OnlineFirst July 17, 2012; DOI: 10.1158/1940-6207.CAPR-11-0397



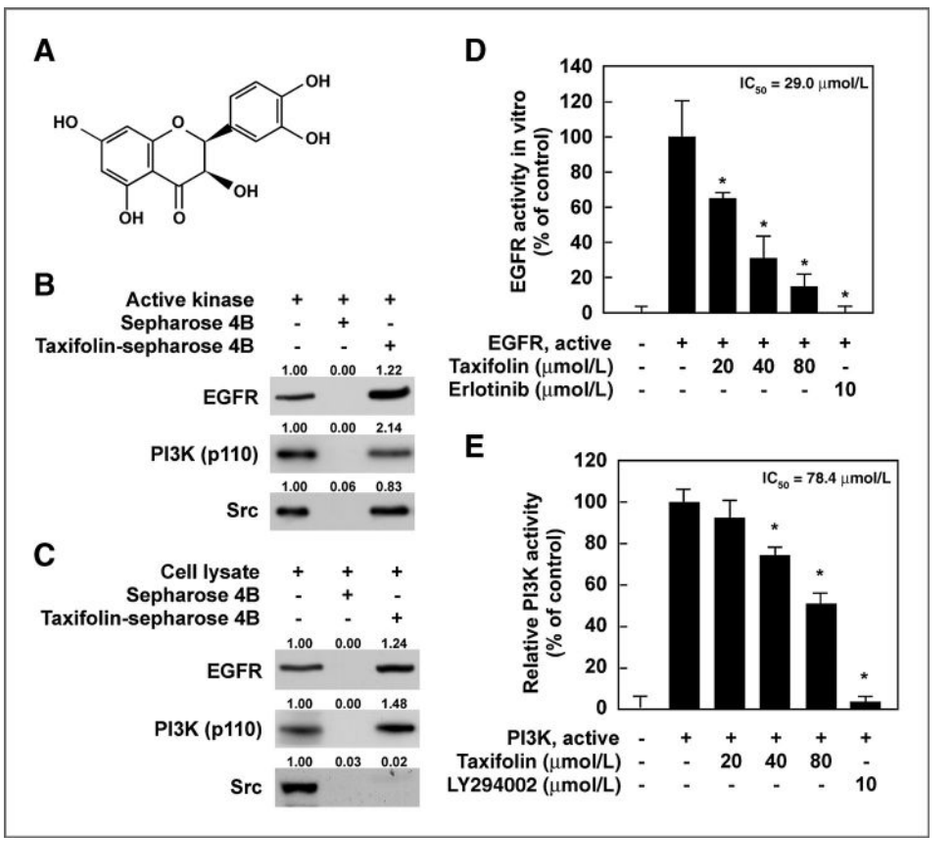


**Figure 1.** EGFR and PI3K are important targets of taxifolin. A, chemical structure of taxifolin. B, taxifolin binds to EGFR, PI3K, and Src *in vitro*. Active EGFR, PI3K, or Src (200 ng) was incubated with taxifolin-conjugated sepharose 4B beads or sepharose 4B beads alone, and the pulled-down proteins were analyzed by Western blot. C, taxifolin binds to EGFR and PI3K but not to Src *ex vivo*. Cell lysates from JB6 P+ cells (500 μg) were incubated with taxifolin-conjugated sepharose 4B beads or sepharose 4B beads, and the pulled-down proteins were analyzed by Western blot. Data are representative of 3 independent experiments that gave similar results. D, taxifolin inhibits EGFR kinase activity *in vitro*. Active EGFR (100 ng) was mixed with taxifolin (0, 20, 40, or 80 μmol/L) or erlotinib (EGFR inhibitor, 10 μmol/L) and then incubated with an [γ-$^{32}$P] ATP mixture. The radioactive incorporation was determined using a scintillation counter. E, taxifolin inhibits PI3K activity *in vitro*. Active PI3K (100 ng) was mixed with taxifolin (0, 20, 40, or 80 μmol/L) or LY294002 (PI3K inhibitor, 10 μmol/L) and then incubated with an [γ-$^{32}$P] ATP mixture. The $^{32}$P-labeled PI3P was separated by thin-layer chromatography and then visualized by autoradiography. Data are represented as mean ± SD from 3 independent experiments conducted with triplicate samples and significance was determined by the Student *t* test. The asterisk (*) indicates a significant decrease versus EGFR or PI3K alone ($P < 0.05$).

of compound together with 1 ng/mL EGF. After incubation for 7 days in a $CO_2$ incubator, colonies were counted.

### Animals

Female SKH-1 hairless mice (5–13 weeks old) were purchased from Charles River. Animals were acclimated for 2 weeks before the study and had free access to food and water. All animal studies were conducted according to the guidelines approved by the University of Minnesota Institutional Animal Care and Use Committee (IACUC). The animals were housed in climate-controlled quarters with a 12-hour light/dark cycle.

Skin carcinogenesis was induced by an SUV irradiation system (SUV-340, Q-LAB). SKH-1 mice were divided into 5 age-matched groups: vehicle group ($n = 10$), 1.0 mg taxifolin group ($n = 10$), Veh/SUV group ($n = 20$), 0.5 mg taxifolin/SUV group ($n = 20$), and 1.0 mg taxifolin/SUV group ($n = 20$). In the vehicle group, 200 μL of acetone was topically treated to the dorsal skin of mice and they were not exposed to SUV. In the 1.0 mg taxifolin group, 1.0 mg taxifolin in 200 μL of acetone was topically treated to the dorsal skin and mice were not exposed to SUV. In the Veh/SUV group, the dorsal skin was topically treated with 200 μL of acetone before SUV irradiation. The mice in the 0.5 mg taxifolin/SUV or 1.0 mg taxifolin/SUV groups received topical application of taxifolin (0.5 or 1.0 mg) in 200 μL of acetone before SUV irradiation. The SUV irradiation was given 3 times a week for 15 weeks as described below. At week 1, mice were irradiated with SUV at a dose of 30 kJ/m$^2$ UVA and 1.8 kJ/m$^2$ UVB 3 times a week. The dose of SUV was progressively increased (10% each week) because of the ensuing hyperplasia that can occur with SUV irradiation of the skin. At week 6, the dose of SUV reached 48 kJ/m$^2$ (UVA) and 2.9 kJ/m$^2$ (UVB) and this dose was maintained for 6 to 15 weeks. Mice were weighed and tumors were measured by caliper once a week until week 30 or tumors reached 1 cm$^3$ total volume, at which time mice were euthanized and then skins were collected for further analysis.

Published OnlineFirst July 17, 2012; DOI: 10.1158/1940-6207.CAPR-11-0397



### Statistical analysis

All quantitative data are expressed as mean ± SD or SE as indicated. The Student *t* test or a one-way ANOVA was used for statistical analysis. A probability of $P < 0.05$ was used as the criterion for statistical significance.

## Results

### EGFR and PI3K are potential targets of taxifolin

To find potential molecular targets of taxifolin (Fig. 1A), we first conducted *in silico* screening using a shape similarity method. Shape similarity scores of 15 proteins were more than 0.7, suggesting that those proteins are potential targets of taxifolin (Supplementary Table S1). We then conducted *in vitro* kinase profiling (KinaseProfiler; Millipore) with taxifolin against those proteins. Results indicated that the kinase activities of EGFR, PI3K, and Src were inhibited by more than 50% by taxifolin at 80 μmol/L (EGFR, 95%; PI3K, 51%; and Src, 53%, respectively). To determine whether taxifolin binds to EGFR, PI3K, or Src, *in vitro* and *ex vivo* pull-down assays were conducted. Recombinant EGFR, PI3K, and Src indeed interacted with taxifolin-sepharose 4B beads *in vitro* (Fig. 1B). However, taxifolin-sepharose 4B beads pulled down only EGFR and PI3K, but not Src using cell lysates from JB6 P+ cells *ex vivo* (Fig. 1C). *In vitro* kinase assay results revealed that taxifolin suppressed kinase activities of EGFR (Fig. 1D) and PI3K (Fig. 1E), and the $IC_{50}$ value of taxifolin against EGFR or PI3K was 29.0 or 78.4 μmol/L, respectively. These results indicate that EFGR and PI3K are effective targets of taxifolin.

### Taxifolin binds to EGFR and PI3K at the ATP-binding pocket

Our computer screening indicated that the shape and pharmacophore of taxifolin were similar with *N*-[4-(3-bromo-phenylamino)-quinazolin-6-yl]-acrylamide (PDB ID: 2j5f), a known EGFR inhibitor, and with 4-amino-2-methyl-*N*-(1H-pyrazol-3-yl) quinazoline-8-carboxamide (PDB ID: 3prz), a known PI3K inhibitor (Supplementary Table S1). Both inhibitors were reported to interact with the ATP-binding pocket of the respective proteins.

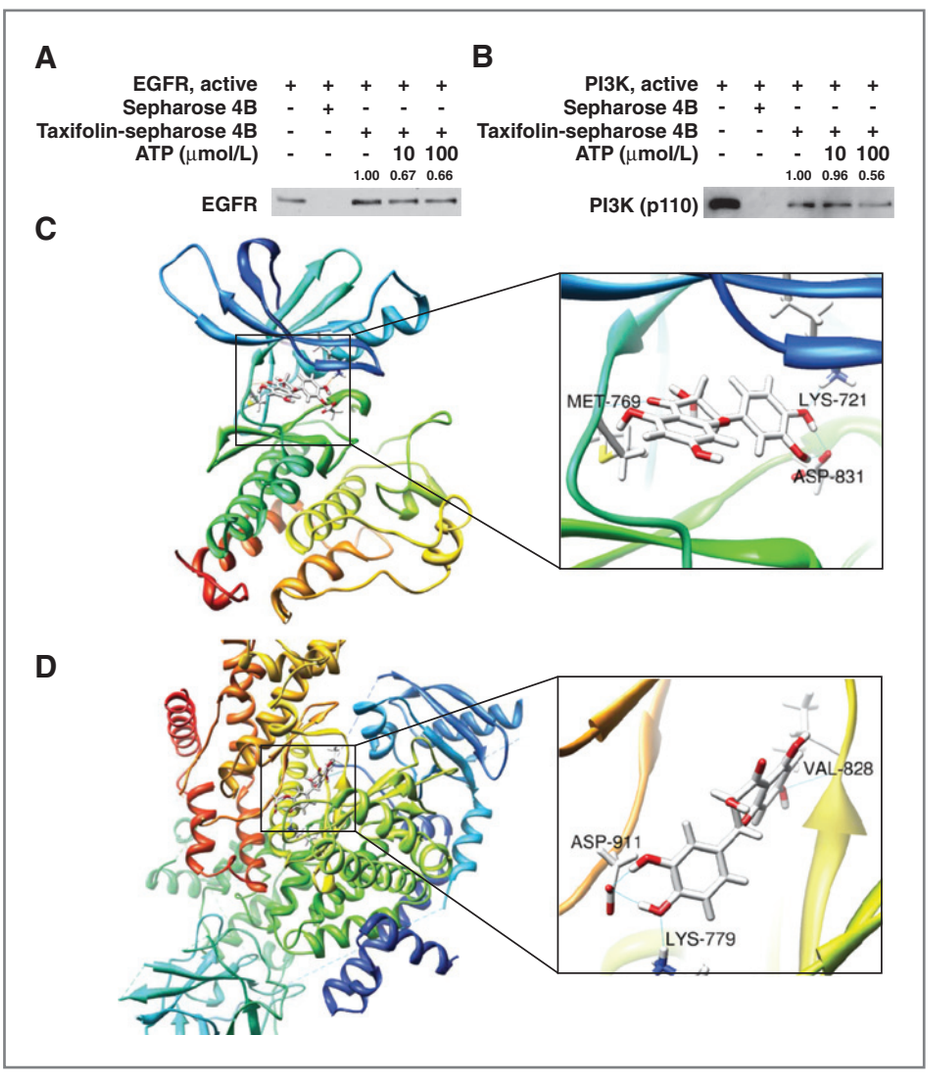


Figure 2. Taxifolin binds to EGFR and PI3K at the ATP-binding pocket. A, taxifolin binds with EGFR in an ATP-competitive manner. B, taxifolin binds with PI3K in an ATP-competitive manner. Active EGFR or PI3K (200 ng) was incubated with different concentrations of ATP (0, 10, or 100 μmol/L) and then incubated with taxifolin-conjugated sepharose 4B beads or sepharose 4B beads. The pulled down proteins were analyzed by Western blot analysis. Data are representative of 3 independent experiments that gave similar results. C, docking model of EGFR and taxifolin. D, docking model of PI3K and taxifolin. Docking models show the predicted interactions.

Published OnlineFirst July 17, 2012; DOI: 10.1158/1940-6207.CAPR-11-0397



Therefore, taxifolin might also bind to the ATP-binding pocket. ATP competition assays showed that the binding ability of taxifolin with EGFR (Fig. 2A) or PI3K (Fig. 2B) was altered in the presence of ATP. We then docked taxifolin to EGFR or PI3K using the Induced Fit Docking module of the Schrödinger Suite 2010 in extra precision. Taxifolin formed interactions within the ATP-binding pocket of EGFR (Fig. 2C) or PI3K (Fig. 2D). The important hydrogen bonds with taxifolin were formed with Lys721, Met769, and Asp831 of EGFR and Lys779, Val828, and Asp911 of PI3K, respectively. These results suggest that taxifolin is an ATP-competitive inhibitor of EGFR and PI3K.

### Taxifolin suppresses UVB-induced EGFR and PI3K/Akt signaling pathways in JB6 P+ cells

To show the effect of taxifolin on UV-induced skin carcinogenesis, we first determined the cytotoxicity of taxifolin in the JB6 P+ mouse epidermal cell line. Taxifolin up to 80 μmol/L had no cytotoxicity in JB6 P+ cells (Fig. 3A). Gefitinib, a well-known selective EGFR inhibitor, is reported to interact with EGFR at the ATP-binding pocket and suppresses EGFR kinase activity by attenuation of its autophosphorylation (35). According to our results showing that taxifolin binds to EGFR at the ATP-binding site (Fig. 2A, C), taxifolin might also suppress autophosohorylation of EGFR. In fact, UVB-induced phosphorylation of EGFR at Tyr1068, which is an important autophosphorylation site of EGFR, is suppressed by taxifolin (Fig. 3B). Phosphorylation of Akt and p70S6K, PI3K/Akt signaling proteins, was also suppressed by taxifolin (Fig. 3C). We then determined whether taxifolin could inhibit UVB-induced phosphorylation of ERKs, p38, and JNKs, well-known signaling kinases phosphorylated by EGFR in response to UV irradiation (14–16). Taxifolin suppressed UVB-induced phosphorylation of ERKs, p38, and JNKs (Fig. 3D) and also reduced phosphorylation of their downstream target proteins, p90RSK, MSK, and c-Jun (Fig. 3E). To confirm that the effects of taxifolin on these signaling proteins are related to the inhibition of EGFR and PI3K, we used gefitinib or LY294002 as positive controls (Fig. 3C–E). Gefitinib suppressed phosphorylation of all the kinases induced by UVB including those in the PI3K/Akt signaling pathway because EGFR also activates PI3K/Akt signaling in response to UV irradiation (11, 24). LY294002 only

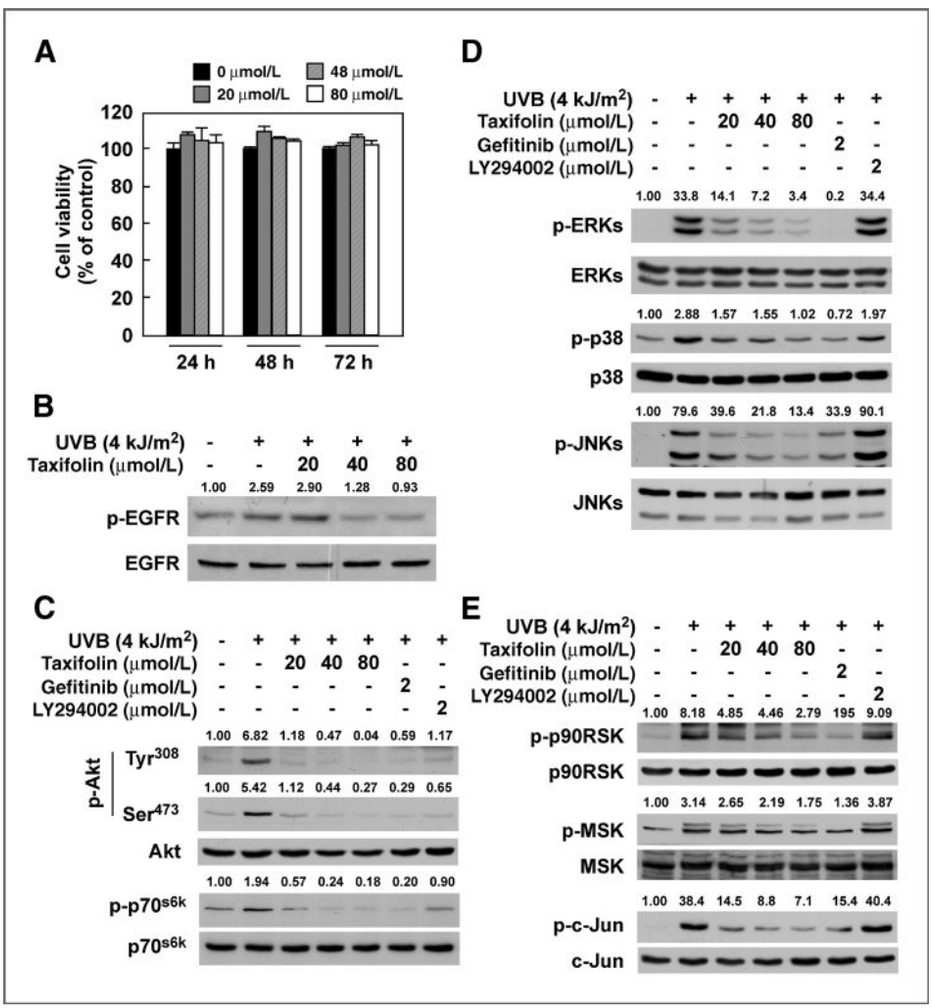


Figure 3. Taxifolin suppresses UVB-induced phosphorylation of the EGFR and PI3K/Akt signaling pathways. A, taxifolin has no toxicity on JB6 P+ cells. JB6 P+ cells were treated with taxifolin (0, 20, 40, or 80 μmol/L) for 24, 48, or 72 hours. Data are represented as mean ± SD from 3 independent experiments conducted with triplicate samples and significance was determined by the Student *t* test. No significant difference was observed between any groups. B, taxifolin inhibits UVB-induced phosphorylation of EGFR. C, taxifolin inhibits UVB-induced phosphorylation of PI3K/Akt signaling proteins. D, taxifolin inhibits UVB-induced phosphorylation of ERKs, p38, and JNKs. E, taxifolin inhibits UVB-induced phosphorylation of p90RSK, MSK, and c-Jun. B–E, JB6 P+ cells were starved in serum-free MEM and treated with taxifolin (0, 20, 40, or 80 μmol/L), gefitinib (2 μmol/L), or LY294002 (2 μmol/L) for 24 hours before being exposed to UVB (4 kJ/m$^2$). After incubation for 5 minutes (B), 15 minutes (C and D), or 30 minutes (E), cells were harvested and the levels of phosphorylated and total proteins were determined by Western blot analysis. Data are representative of 3 independent experiments that gave similar results.

Published OnlineFirst July 17, 2012; DOI: 10.1158/1940-6207.CAPR-11-0397



suppressed phosphorylation of the PI3K/Akt signaling pathway. These data suggest that taxifolin suppresses UVB-induced activation of the EGFR and PI3K/Akt signaling pathways through inhibition of EGFR and PI3K.

### Taxifolin suppresses UVB-induced COX-2 through EGFR and PI3K/Akt signaling in JB6 P+ cells

The EGFR, as well as the PI3K/Akt signaling pathways, are reported to enhance expression levels of COX-2 in response to UV irradiation (36–37). We therefore examined whether taxifolin could suppress UV-induced COX-2 expression and found that taxifolin suppressed UVB-induced COX-2 expression in a dose-dependent manner (Fig. 4A). Gefitinib and LY294002 suppressed COX-2 expression and cotreatment with gefitinib, and LY294002 showed a stronger effect than treatment individually (Fig. 4A). Taxifolin also suppressed UVB-induced promoter activity of *COX-2* (Fig. 4B) and generation of $PGE_2$ (Fig. 4C), the enzyme product of COX-2, in JB6 P+ cells. To verify that taxifolin does not inhibit COX-2 directly, *in vitro* COX-2 activity was determined and results indicated that taxifolin had no effect on COX-2 activity *in vitro* (Fig. 4D). These results suggest that taxifolin regulates COX-2 through inhibition of EGFR and PI3K.

### The effect of taxifolin is reduced in EGFR/KO MEFs compared with EGFR/WT MEFs

Our *in vitro* kinase assay data showed that the $IC_{50}$ values of taxifolin are 29.0 μmol/L for EGFR and 78.4 μmol/L for PI3K, respectively (Fig. 1D and E), suggesting that EGFR is the major target of taxifolin. We therefore compared the effects of taxifolin in EGFR/WT and KO MEFs. Western blotting data verified that EGFR was only detected in EGFR/WT MEFs (Fig. 5A). Taxifolin suppressed UVB-induced phosphorylation of ERKs, p38, JNKs, and Akt in EGFR/WT MEFs, whereas the effects of taxifolin on phosphorylation of ERKs, p38, and JNKs were not apparent in EGFR/KO MEFs (Fig. 5B). Phosphorylation of Akt was completely blocked in EGFR/KO MEFs and UVB-induced $PGE_2$ generation was strongly downregulated by knocking down EGFR expression (Fig. 5C). The effect of taxifolin on UVB-induced $PGE_2$

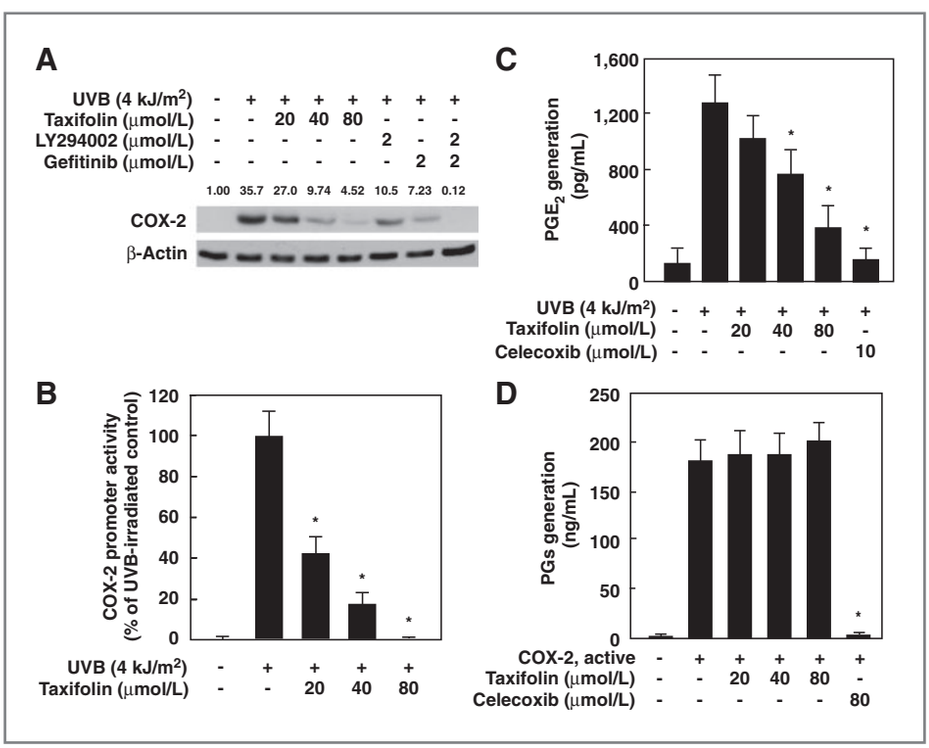


Figure 4. Taxifolin suppresses UVB-induced expression and promoter activity of *COX-2* and $PGE_2$ generation. A, taxifolin, as well as inhibitors of EGFR or PI3K, suppress UVB-induced COX-2 expression. Cells were starved in serum-free MEM and then treated with taxifolin (0, 20, 40, or 80 μmol/L), gefitinib (2 μmol/L), and/or LY294002 (2 μmol/L) for 24 hours before being exposed to UVB (4 kJ/m$^2$). After incubation for 4 hours, the cells were harvested and the levels of COX-2 and β-actin were determined. Data are representative of 3 independent experiments that gave similar results. B, taxifolin suppresses the promoter activity of *COX-2* induced by UVB. JB6 P+ cells stably transfected with a *COX-2* luciferase reporter plasmid were starved in serum-free medium and then treated with taxifolin (0, 20, 40, or 80 μmol/L) for 1 hour before exposure to UVB (4 kJ/m$^2$). After incubation for 12 hours, luciferase activity was measured. C, taxifolin suppresses $PGE_2$ generation induced by UVB. Cells were starved in serum-free MEM and then treated with taxifolin (0, 20, 40, or 80 μmol/L) or celecoxib (COX-2 inhibitor, 10 μmol/L) for 1 hour before being exposed to UVB (4 kJ/m$^2$). After incubation for 6 hours, $PGE_2$ generation in the medium was determined using a $PGE_2$ EIA kit. D, taxifolin has no effect on COX-2 activity *in vitro*. *In vitro* COX-2 activity was determined using the COX Inhibitor Screening Assay kit. B–D, data are represented as mean ± SD from 3 independent experiments carried out with triplicate samples and significance was determined by the Student *t* test. The asterisk (*) indicates a significant decrease versus UVB (B and C) or COX-2 (D) alone ($P < 0.05$).

Published OnlineFirst July 17, 2012; DOI: 10.1158/1940-6207.CAPR-11-0397



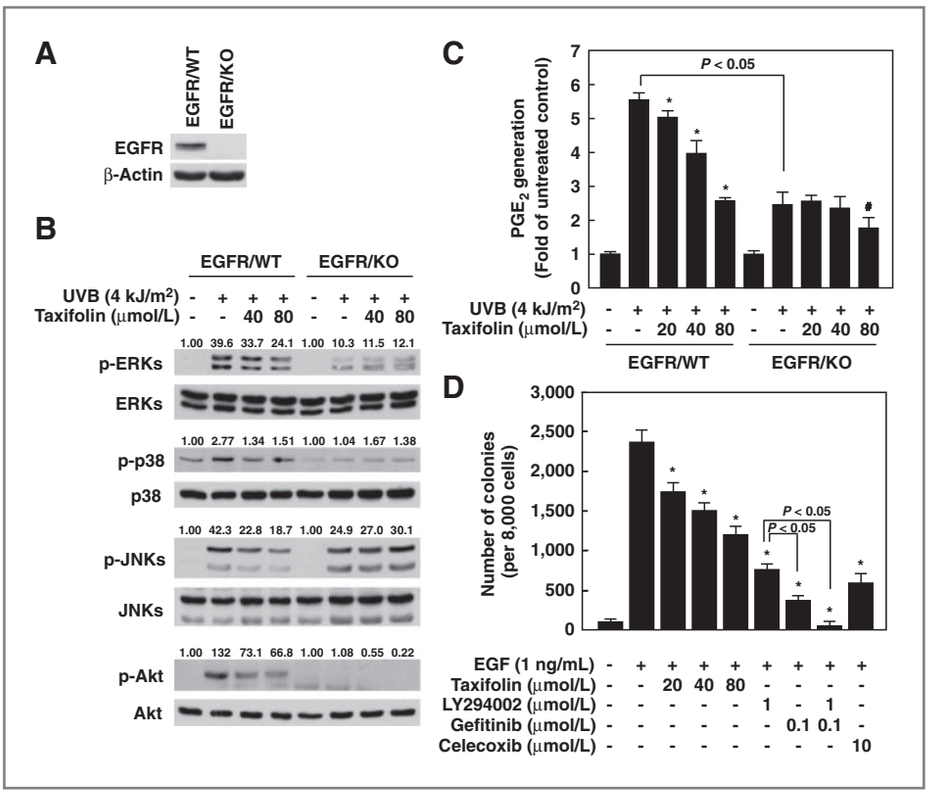


**Figure 5.** The effect of taxifolin was reduced in EGFR/KO MEFs compared with EGFR/WT MEFs. A, EGFR expression is only detectable in EGFR/WT MEFs. B, the effect of taxifolin on UVB-induced phosphorylation of signaling proteins is reduced in EGFR/KO MEFs compared with EGFR/WT MEFs. EGFR/WT or KO MEFs were starved in serum-free DMEM and then treated with taxifolin (0, 40, or 80 μmol/L) for 24 hours before being exposed to UVB (4 kJ/m$^2$). After incubation for 15 minutes, the cells were harvested and the levels of phosphorylated and total proteins were determined by Western blot analysis. A and B, data are representative of 3 independent experiments that gave similar results. C, the effect of taxifolin on $PGE_2$ generation is reduced in EGFR/KO MEFs compared with EGFR/WT MEFs. EGFR/WT or KO MEFs were starved in serum-free DMEM and then treated with taxifolin (0, 20, 40, or 80 μmol/L) for 1 hour before being exposed to UVB (4 kJ/m$^2$). After incubation for 6 hours, $PGE_2$ generation in the medium was determined using a $PGE_2$ EIA kit. Data are represented as mean ± SD from 3 independent experiments carried out with triplicate samples and significance was determined by the Student *t* test. The asterisk (*) or (#) indicates a significant decrease versus UVB alone in EGFR/WT or KO MEFs, respectively ($P < 0.05$). D, taxifolin, as well as inhibitors of EGFR, PI3K, or COX-2 suppresses EGF-induced cell transformation. JB6 P+ cells were treated with taxifolin (0, 20, 40, or 80 μmol/L), gefitinib (0.1 μmol/L), LY294002 (1 μmol/L), or celecoxib (10 μmol/L) together with 1 ng/mL EGF on solidified BME supplemented with 10% FBS and 0.5% agar. After incubation for 7 days, colonies were counted. Data are represented as mean ± SD from 3 independent experiments carried out with triplicate samples and significance was determined by the Student *t* test. The asterisk (*) indicates a significant decrease versus EGF alone ($P < 0.05$).

generation was also not obvious in EGFR/KO MEFs compared with EGFR/WT MEFs (Fig. 5C). These results suggest that EGFR is a major target of taxifolin in UVB-induced skin carcinogenesis. The UV spectrum can be divided into UVA (320–400 nm), UVB (280–320 nm), and UVC (200–280 nm; refs. 3, 4). Because the UV spectrum ($\lambda_{max}$) of taxifolin is 289 ± 2 nm, at least a portion of the effect of taxifolin could be due to UV absorption. To address this issue, we determined whether taxifolin could inhibit EGF-induced cell transformation, and results indicated that taxifolin suppressed EGF-induced cell transformation (Fig. 5D). Gefitinib and LY294002, as well as celecoxib, also suppressed EGF-induced cell transformation and cotreatment with gefitinib and LY294002 showed a stronger effect than individual drug treatment. These results indicate that taxifolin also suppresses cell transformation induced by EGFR stimulation and not only affects the UV-induced signaling pathways.

### Taxifolin suppresses SUV-induced skin carcinogenesis in SKH-1 hairless mice *in vivo*

To investigate the chemopreventive effect of taxifolin *in vivo*, we used the SUV-induced skin carcinogenesis mouse model. Although UVB is a major etiologic factor for the development of skin cancer, UVA is the most abundant component of UV irradiation (4). SUV irradiation consists of UVA and UVB and more closely resembles the natural environment than UVB only. At first, we confirmed that taxifolin indeed suppressed SUV-induced COX-2 expression (Supplementary Fig. S2A) and $PGE_2$ generation (Supplementary Fig. S2B). We then investigated the chemopreventive effect of taxifolin in the SUV-induced skin carcinogenesis mouse model. Topical

Published OnlineFirst July 17, 2012; DOI: 10.1158/1940-6207.CAPR-11-0397



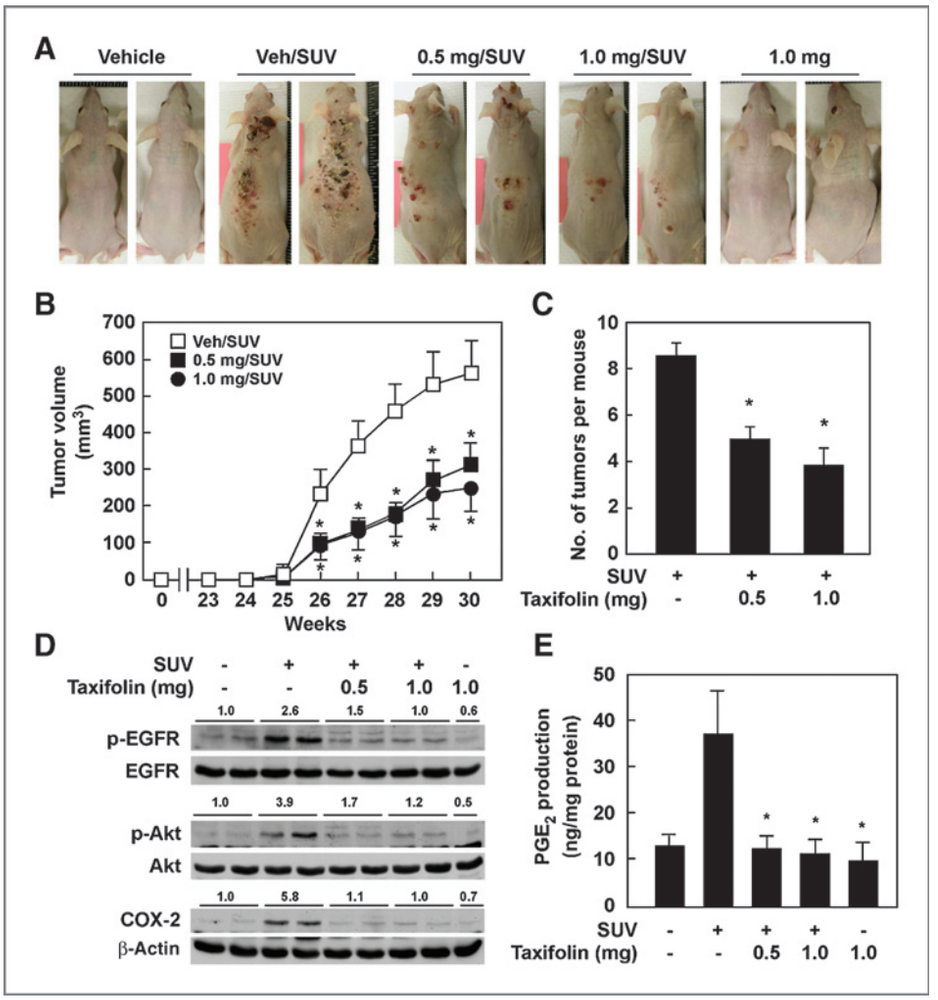


Figure 6. Taxifolin suppresses SUV-induced skin carcinogenesis *in vivo*. SKH-1 hairless mice were treated as described in Materials and Methods. The mice in the vehicle group ($n = 10$) received topical treatment with acetone only. The mice in the 1.0 mg taxifolin group ($n = 10$) were treated with 1.0 mg taxifolin only. In the Veh/SUV group ($n = 20$), the mice were treated with acetone before SUV exposure. The mice in the 0.5 mg/SUV or 1.0 mg/SUV groups ($n = 20$ each) received treatment with taxifolin (0.5 or 1.0 mg, respectively) before SUV exposure. The frequency of irradiation was set at 3 times a week for 15 weeks. The respective doses of acetone or taxifolin were applied topically to the dorsal area. Tumor incidence and multiplicity were recorded weekly until the end of the experiment at week 30. A, external appearance of tumors. B, taxifolin suppresses SUV-induced tumor volume. Tumor volume was calculated according to the following formula: tumor volume ($mm^3$) = length × width × height × 0.52. C, taxifolin suppresses SUV-induced tumor number per mouse at the end of experiment (week 30). B and C, data are represented as mean ± SE and differences were determined by one-way ANOVA. The asterisk (*) indicates a significant decrease versus the Veh/SUV group ($P < 0.01$). D, taxifolin inhibits SUV-induced phosphorylation of EGFR and Akt and COX-2 expression in mouse skin. The expression levels of phosphorylated and total proteins were analyzed by Western blot analysis. E, taxifolin suppresses SUV-induced $PGE_2$ production in mouse skin. $PGE_2$ production was determined using a $PGE_2$ EIA kit, and the amount of $PGE_2$ is expressed as ng/mg protein. D and E, data are represented as mean ± SD and significance was determined by the Student *t* test. The asterisk (*) indicates a significant decrease versus SUV alone ($P < 0.05$).

application of taxifolin on mouse skin resulted in a substantial inhibition of SUV-induced tumor incidence (Fig. 6A). Topical application of taxifolin decreased the average tumor volume per mouse (Fig. 6B) and also significantly reduced tumor multiplicity at week 30 (Fig. 6C). Western blot analysis of the mouse skin showed that phosphorylation of EGFR and Akt and COX-2 expression induced by SUV were dramatically suppressed in the taxifolin-treated group (Fig. 6D). Taxifolin also strongly suppressed SUV-induced $PGE_2$ generation in mouse skin (Fig. 6E). These results clearly showed that taxifolin exerts a strong preventive effect against SUV-induced mouse skin carcinogenesis through the inhibition of EGFR and PI3K activation.

## Discussion

Taxifolin has been reported to exert chemopreventive effects on several cancers. However, the mechanism and direct targets of taxifolin have not been elucidated. In the present study, we report that taxifolin directly inhibits the kinase activities of EGFR and PI3K, and exerts strong chemopreventive effects against UV-induced skin carcinogenesis. Several studies have shown that the EGFR and PI3K/Akt signaling pathways are critical for UV-induced skin

Published OnlineFirst July 17, 2012; DOI: 10.1158/1940-6207.CAPR-11-0397



carcinogenesis. EGFR is activated and/or overexpressed in a variety of human cancers including UV-induced skin cancer (9, 10) and AG1478, a specific inhibitor of EGFR, was shown to prevent UV-induced skin carcinogenesis (14). UV-irradiation was also reported to suppress mitochondria- and caspase-dependent apoptosis through the PI3K/Akt pathway and PI3K inhibitors, LY294002 and wartmannin, which suppressed the rescue from apoptosis by UV irradiation (38). Therefore, our finding suggests the usefulness of taxifolin in UV-induced skin cancer prevention by direct inhibition of EGFR and PI3K.

According to our in *sillico* computer screening and kinase profiling data, we identified EGFR, PI3K, and Src as potential targets of taxifolin (Supplementary Table S1). *In vitro* pull-down data showed that taxifolin pulled down EGFR, PI3K, and Src, whereas taxifolin only pulled down EGFR and PI3K when taxifolin was incubated with cell lysates *ex vivo* (Fig. 1B and C). These results suggest that the binding affinity of taxifolin with Src is lower than with EGFR and PI3K. Therefore, we conclude that EGFR and PI3K are targets of taxifolin. The $IC_{50}$ value of taxifolin against those kinase activities *in vitro* was 29.0 μmol/L for EGFR and 78.4 μmol/L for PI3K, respectively (Fig. 1D and E). The effect of taxifolin on UV-induced phosphorylation of ERKs, JNKs, and p38 completely disappeared in EGFR/ KO MEFs (Fig. 5B), and inhibition of UV-induced $PGE_2$ generation by taxifolin were also not apparent in EGFR/ KO MEFs (Fig. 5C). These results suggest that EGFR is a major effective target of taxifolin.

Taxifolin is found in an aglycone or glycoside form at different levels in various plants, including onions (18), milk thistle (19), French maritime bark (20), and Douglas fir bark (21). For example, the aglycon form was extracted at 97.1 mg/kg and the taxifolin-7-gluoside form at 5.8 mg/kg from the bulbs of red onion (18), and very high levels of the aglycon form (620 mg/kg) are found in the seed of milk thistle (19). Because taxifolin has 2 chiral carbon centers, 4 enantiomeric forms of taxifolin are possible, 2*S*3*R*-(+), 2*S*3*S*-(−), 2*R*3*R*-(+), and 2*R*3*S*-(−)-taxifolin (39). Many studies that have considered enantioseparation of taxifolin did not separate the 4 enantiomers, but only 2 enantiomers (39–41). Vega-Villa and colleagues (39) successfully separated 4 enantiomers of taxifolin and their glycosides using reversed-phase high-performance liquid chromatography. They indicated that 2*R*3*R*-(+)-taxifolin is a major taxifolin enantiomer in tu fu ling (*Rhizoma smilacis glabrae*), which has been used in traditional Chinese medicine to treat patients with cancer and AIDS (42). Engelhardtia chrysolepis, which is also a traditional Chinese medicine, mainly contains 2*R*3*R*-(+)-taxifolin as astilbin (2*R*3*R*-(+)-taxifolin rhamnoside; ref. 22). In the present study, we used 2*R*3*R*-(+)-taxifolin for *in vitro* and cell-based experiments, and (+)-taxifolin (2*R*3*R*, 2*S*3*R*-(+)-taxifolin) for the *in vivo* study. The purities of 2*R*3*R*-(+)-taxifolin and (+)-taxifolin are 85% and 90%, respectively. These low purities are because of the difficulty of separation of 4 taxifolin enantiomers. We therefore compared the docking score of each of the 4 taxifolin enantiomers against EGFR or PI3K by computer modeling. All 4 taxifolin enantiomers interact with EGFR and PI3K with a similar docking score (Supplementary Table S2). We therefore conclude that even though taxifolin enantiomers are probably contaminants, these enantiomers likely also have the ability to inhibit the kinase activity of EGFR or PI3K.

Our results showed that taxifolin suppressed UVB-induced phosphorylation of EGFR signaling as well as the PI3K/Akt signaling pathways (Fig 3B–E). Previous studies indicate that UV-induced EGFR and PI3K/Akt signaling pathways play important regulatory roles in COX-2 expression and $PGE_2$ generation (36–37). COX-2, a rate-limiting enzyme for oxidative conversion of arachidonic acid to PGs, is recognized as a critical enzyme for enhancing cell proliferation, angiogenesis, and tumor promotion (2, 43). In human and murine skin cells, COX-2 is upregulated in response to acute and chronic UVB irradiation (37), and a selective COX-2 inhibitor strongly suppresses UV-induced skin carcinogenesis (44). Importantly, direct inhibitors of EGFR or PI3K reduce UVB-induced skin carcinogenesis by downregulation of COX-2 expression (36). We therefore investigated whether the inhibition of EGFR and PI3K/Akt pathways by taxifolin affects COX-2 expression. Our results indicated that UVB-induced COX-2 expression and $PGE_2$ generation were suppressed by taxifolin (Fig. 4A and B). Consistent with previous reports, selective inhibitors of EGFR or PI3K showed strong inhibition of UVB-induced COX-2 expression. These results suggest that taxifolin suppresses UV-induced COX-2 expression by inhibition of EGFR and PI3K. Wang and colleagues (24) reported that taxifolin suppressed lipopolysaccharide (LPS)-induced COX-2 expression. However, no information regarding the direct target of taxifolin was included. LPS is reported to mediate enhanced COX-2 expression through the activation of EGFR (45). Sheu and colleagues also showed that the PI3K/Akt signaling pathway is involved in COX-2 expression and cell proliferation induced by LPS (46). These reports support our finding that taxifolin suppresses COX-2 expression through inhibition of EGFR and PI3K. Overall, our study showed that taxifolin exerted excellent inhibitory effects against UV-induced skin by directly targeting EGFR and PI3K. Thus, taxifolin is expected to have highly beneficial effects in the prevention of skin carcinogenesis.

## Disclosure of Potential Conflicts of Interest

No potential conflicts of interest were disclosed.

## Authors' Contributions

**Conception and design:** N. Oi, M.O. Kim, Z. Dong
**Development of methodology:** N. Oi, M.O. Kim, R.A. Lubet, Z. Dong
**Acquisition of data (provided animals, acquired and managed patients, provided facilities, etc.):** N. Oi, M.O. Kim, Z. Dong
**Analysis and interpretation of data (e.g., statistical analysis, biostatistics, computational analysis):** N. Oi, H. Chen, M.O. Kim, R.A. Lubet, A.M. Bode, Z. Dong
**Writing, review, and/or revision of the manuscript:** N. Oi, H. Chen, M.O. Kim, R.A. Lubet, A.M. Bode, Z. Dong
**Administrative, technical, or material support (i.e., reporting or organizing data, constructing databases):** N. Oi, Z. Dong
**Study supervision:** A.M. Bode, Z. Dong
**Computational method and modeling:** H. Chen

Published OnlineFirst July 17, 2012; DOI: 10.1158/1940-6207.CAPR-11-0397



## Grant Support

This work was supported by the Hormel Foundation and NI H grants R37 CA081064, CA027502, CA120388, and ES016548.

The costs of publication of this article were defrayed in part by the payment of page charges. This article must therefore be hereby marked *advertisement* in accordance with 18 U.S.C. Section 1734 solely to indicate this fact.

Received August 10, 2011; revised May 30, 2012; accepted June 16, 2012; published OnlineFirst July 17, 2012.

## References

1. Ricotti C, Bouzari N, Agadi A, Cockerell CJ. Malignant skin neoplasms. Med Clin North Am 2009;93:1241–64.
2. Buckman SY, Gresham A, Hale P, Hruza G, Anast J, Masferrer J, et al. COX-2 expression is induced by UVB exposure in human skin: implications for the development of skin cancer. Carcinogenesis 1998;19:723–9.
3. de Gruijl FR. Photocarcinogenesis: UVA vs UVB. Methods Enzymol 2000;319:359–66.
4. Matsui MS, DeLeo VA. Longwave ultraviolet radiation and promotion of skin cancer. Cancer Cells 1991;3:8–12.
5. Nichols JA, Katiyar SK. Skin photoprotection by natural polyphenols: anti-inflammatory, antioxidant and DNA repair mechanisms. Arch Dermatol Res 2010;302:71–83.
6. Bode AM, Dong Z. Mitogen-activated protein kinase activation in UV-induced signal transduction. Sci STKE 2003;2003:RE2.
7. Matsumura Y, Ananthaswamy HN. Toxic effects of ultraviolet radiation on the skin. Toxicol Appl Pharmacol 2004;195:298–308.
8. Rosette C, Karin M. Ultraviolet light and osmotic stress: activation of the JNK cascade through multiple growth factor and cytokine receptors. Science 1996;274:1194–7.
9. Gullick WJ. Prevalence of aberrant expression of the epidermal growth factor receptor in human cancers. Br Med Bull 1991;47:87–98.
10. Scaltriti M, Baselga J. The epidermal growth factor receptor pathway: a model for targeted therapy. Clin Cancer Res 2006;12:5268–72.
11. Coffer PJ, Burgering BM, Peppelenbosch MP, Bos JL, Kruijer W. UV activation of receptor tyrosine kinase activity. Oncogene 1995;11:561–9.
12. Huang RP, Wu JX, Fan Y, Adamson ED. UV activates growth factor receptors via reactive oxygen intermediates. J Cell Biol 1996;133:211–20.
13. Xu Y, Shao Y, Voorhees JJ, Fisher GJ. Oxidative inhibition of receptor-type protein-tyrosine phosphatase kappa by ultraviolet irradiation activates epidermal growth factor receptor in human keratinocytes. J Biol Chem 2006;281:27389–97.
14. El-Abaseri TB, Fuhrman J, Trempus C, Shendrik I, Tennant RW, Hansen LA. Chemoprevention of UV light-induced skin tumorigenesis by inhibition of the epidermal growth factor receptor. Cancer Res 2005;65:3958–65.
15. El-Abaseri TB, Putta S, Hansen LA. Ultraviolet irradiation induces keratinocyte proliferation and epidermal hyperplasia through the activation of the epidermal growth factor receptor. Carcinogenesis 2006;27:225–31.
16. Peus D, Vasa RA, Meves A, Beyerle A, Pittelkow MR. UVB-induced epidermal growth factor receptor phosphorylation is critical for downstream signaling and keratinocyte survival. Photochem Photobiol 2000;72:135–40.
17. Wan YS, Wang ZQ, Shao Y, Voorhees JJ, Fisher GJ. Ultraviolet irradiation activates PI 3-kinase/AKT survival pathway via EGF receptors in human skin *in vivo*. Int J Oncol 2001;18:461–6.
18. Slimestad R, Fossen T, Vagen IM. Onions: a source of unique dietary flavonoids. J Agric Food Chem 2007;55:10067–80.
19. Wallace SN, Carrier DJ, Clausen EC. Batch solvent extraction of flavanolignans from milk thistle (Silybum marianum L. Gaertner). Phytochem Anal 2005;16:7–16.
20. Rohdewald P. A review of the French maritime pine bark extract (Pycnogenol), a herbal medication with a diverse clinical pharmacology. Int J Clin Pharmacol Ther 2002;40:158–68.
21. Kiehlmann E, Li EPM. Isomerization of dihydroquercetin. J Nat Products 1995;58:450–5.
22. Haraguchi H, Mochida Y, Sakai S, Masuda H, Tamura Y, Mizutani K, et al. Protection against oxidative damage by dihydroflavonols in *Engelhardtia chrysolepis*. Biosci Biotechnol Biochem 1996;60:945–8.
23. Kostyuk VA, Kraemer T, Sies H, Schewe T. Myeloperoxidase/nitrite-mediated lipid peroxidation of low-density lipoprotein as modulated by flavonoids. FEBS Lett 2003;537:146–50.
24. Wang YH, Wang WY, Chang CC, Liou KT, Sung YJ, Liao JF, et al. Taxifolin ameliorates cerebral ischemia-reperfusion injury in rats through its anti-oxidative effect and modulation of NF-kappa B activation. J Biomed Sci 2006;13:127–41.
25. Lee SB, Cha KH, Selenge D, Solongo A, Nho CW. The chemopreventive effect of taxifolin is exerted through ARE-dependent gene regulation. Biol Pharm Bull 2007;30:1074–9.
26. Brusselmans K, Vrolix R, Verhoeven G, Swinnen JV. Induction of cancer cell apoptosis by flavonoids is associated with their ability to inhibit fatty acid synthase activity. J Biol Chem 2005;280:5636–45.
27. Jung SK, Lee KW, Byun S, Kang NJ, Lim SH, Heo YS, et al. Myricetin suppresses UVB-induced skin cancer by targeting Fyn. Cancer Res 2008;68:6021–9.
28. Bode AM, Cho YY, Zheng D, Zhu F, Ericson ME, Ma WY, et al. Transient receptor potential type vanilloid 1 suppresses skin carcinogenesis. Cancer Res 2009;69:905–13.
29. Schrödinger. Schrödinger Suite 2010. New York: Schrödinger, LLC; 2010.
30. Berman HM, Westbrook J, Feng Z, Gilliland G, Bhat TN, Weissig H, et al. The Protein Data Bank. Nucleic Acids Res 2000;28:235–42.
31. Kwon JY, Lee KW, Kim JE, Jung SK, Kang NJ, Hwang MK, et al. Delphinidin suppresses ultraviolet B-induced cyclooxygenases-2 expression through inhibition of MAPKK4 and PI-3 kinase. Carcinogenesis 2009;30:1932–40.
32. Stamos J, Sliwkowski MX, Eigenbrot C. Structure of the epidermal growth factor receptor kinase domain alone and in complex with a 4-anilinoquinazoline inhibitor. J Biol Chem 2002;277:46265–72.
33. Berndt A, Miller S, Williams O, Le DD, Houseman BT, Pacold JI, et al. The p110 delta structure: mechanisms for selectivity and potency of new PI(3)K inhibitors. Nat Chem Biol 2010;6:117–24.
34. Pettersen EF, Goddard TD, Huang CC, Couch GS, Greenblatt DM, Meng EC, et al. UCSF Chimera–a visualization system for exploratory research and analysis. J Comput Chem 2004;25:1605–12.
35. Wakeling AE, Guy SP, Woodburn JR, Ashton SE, Curry BJ, Barker AJ, et al. ZD1839 (Iressa): an orally active inhibitor of epidermal growth factor signaling with potential for cancer therapy. Cancer Res 2002;62:5749–54.
36. Ashida M, Bito T, Budiyanto A, Ichihashi M, Ueda M. Involvement of EGF receptor activation in the induction of cyclooxygenase-2 in HaCaT keratinocytes after UVB. Exp Dermatol 2003;12:445–52.
37. Chen W, Tang Q, Gonzales MS, Bowden GT. Role of p38 MAP kinases and ERK in mediating ultraviolet-B induced cyclooxygenase-2 gene expression in human keratinocytes. Oncogene 2001;20:3921–6.
38. Ibuki Y, Goto R. Suppression of apoptosis by UVB irradiation: survival signaling via PI3-kinase/Akt pathway. Biochem Biophys Res Commun 2000;279:872–8.
39. Vega-Villa KR, Remsberg CM, Ohgami Y, Yanez JA, Takemoto JK, Andrews PK, et al. Stereospecific high-performance liquid chromatography of taxifolin, applications in pharmacokinetics, and determination in tu fu ling (Rhizoma smilacis glabrae) and apple (Malus x domestica). Biomed Chromatogr 2009;23:638–46.
40. Japon-Lujan R, Luque de Castro MD. Static-dynamic superheated liquid extraction of hydroxytyrosol and other biophenols from alperujo

Published OnlineFirst July 17, 2012; DOI: 10.1158/1940-6207.CAPR-11-0397



(a semisolid residue of the olive oil industry). J Agric Food Chem 2007;55:3629–34.
41. Kiehlmann E, Slade PW. Methylation of dihydroquercetin acetates: synthesis of 5-O-methyldihydroquercetin. J Nat Prod 2003;66:1562–6.
42. Chen L, Yin Y, Yi H, Xu Q, Chen T. Simultaneous quantification of five major bioactive flavonoids in Rhizoma smilacis glabrae by high-performance liquid chromatography. J Pharm Biomed Anal 2007;43:1715–20.
43. Dubois RN, Abramson SB, Crofford L, Gupta RA, Simon LS, Van De Putte LB, et al. Cyclooxygenase in biology and disease. FASEB J 1998;12:1063–73.
44. Pentland AP, Schoggins JW, Scott GA, Khan KN, Han R. Reduction of UV-induced skin tumors in hairless mice by selective COX-2 inhibition. Carcinogenesis 1999;20:1939–44.
45. Kuper C, Beck FX, Neuhofer W. Toll-like receptor 4 activates NF-kappaB and MAP kinase pathways to regulate expression of proinflammatory COX-2 in renal medullary collecting duct cells. Am J Physiol Renal Physiol 2012;302:F38–46.
46. Sheu ML, Chao KF, Sung YJ, Lin WW, Lin-Shiau SY, Liu SH. Activation of phosphoinositide 3-kinase in response to inflammation and nitric oxide leads to the up-regulation of cyclooxygenase-2 expression and subsequent cell proliferation in mesangial cells. Cell Signal 2005;17:975–84.

Published OnlineFirst July 17, 2012; DOI: 10.1158/1940-6207.CAPR-11-0397



Cancer Prevention Research

# Taxifolin Suppresses UV-Induced Skin Carcinogenesis by Targeting EGFR and PI3K

Naomi Oi, Hanyong Chen, Myoung Ok Kim, et al.

*Cancer Prev Res* 2012;5:1103-1114. Published OnlineFirst July 17, 2012.